2010

The Abl and Arg non-receptor tyrosine kinases regulate different zones of stress fiber, focal adhesion, and contractile network localization in spreading fibroblasts

Justin G. Peacock
Yale University

Brian A. Couch
Yale University, bcouch2@unl.edu

Anthony J. Koleske
Yale University, anthony.koleske@yale.edu

Published in final edited form as:
Cytoskeleton (Hoboken). 2010 October ; 67(10): 666–675. doi:10.1002/cm.20479.

The Abl and Arg non-receptor tyrosine kinases regulate different zones of stress fiber, focal adhesion, and contractile network localization in spreading fibroblasts

Justin G. Peacock[1], **Brian A. Couch**[1], and **Anthony J. Koleske**[1,2,3,4]

[1]Department of Molecular Biophysics and Biochemistry, Yale University, New Haven, CT

[2]Department of Neurobiology, Yale University, New Haven, CT

[3]Interdepartmental Neuroscience Program, Yale University, New Haven, CT

Abstract

Directed cell migration requires precise spatial control of F-actin-based leading edge protrusion, focal adhesion (FA) dynamics, and actomyosin contractility. In spreading fibroblasts, the Abl family kinases, Abl and Arg, primarily localize to the nucleus and cell periphery, respectively. Here we provide evidence that Abl and Arg exert different spatial regulation on cellular contractile and adhesive structures. Loss of Abl function reduces FA, F-actin, and phosphorylated myosin light chain (pMLC) staining at the cell periphery, shifting the distribution of these elements more to the center of the cell than in wild-type (WT) and *arg*$^{-/-}$ cells. Conversely, loss of Arg function shifts the distribution of these contractile and adhesion elements more to the cell periphery relative to WT and *abl*$^{-/-}$ cells. Abl/Arg-dependent phosphorylation of p190RhoGAP (p190) promotes its binding to p120RasGAP (p120) to form a functional RhoA GTPase inhibitory complex, which attenuates RhoA activity and downstream pMLC and FA formation. p120 and p190 colocalize both in the central region and at the cell periphery in WT cells. This p120:p190 colocalization redistributes to a more peripheral distribution in *abl*$^{-/-}$ cells and to a more centralized distribution in *arg*$^{-/-}$ cells, and these altered distributions can be restored to WT patterns via re-expression of Abl or Arg, respectively. Thus, the altered p120:p190 distribution in the mutant cells correlates inversely with the redistribution in adhesions, actin, and pMLC staining in these cells. Our studies suggest that Abl and Arg exert different spatial regulation on actomyosin contractility and focal adhesions within cells.

Keywords

p190RhoGAP; p120RasGAP; actomyosin contractility; phosphorylated myosin II light chain; and paxillin

Introduction

Cell migration in response to chemotactic and haptotactic cues is essential for proper organismal development [Cantley, 1996; Gilbert, 2003; Ridley et al., 2003]. Dysregulation of cell migration can lead to developmental disorders and diseases, including cancer invasion and metastasis [Friedl et al., 1998; Gilbert, 2003; Hatten, 1999; Schmitz et al., 2000; Simons and Mlodzik, 2008; Watanabe et al., 2005; Yang and Weinberg, 2008]. Directed cell migration is regulated through the integrated function of cell surface receptors,

[4]Corresponding author: anthony.koleske@yale.edu; phone: (203) 785-5624; fax (203) 785-7979.

numerous signaling proteins, the cytoskeleton, and cell adhesion systems [Broussard et al., 2008; Elbaum et al., 1999; Friedl and Gilmour, 2009; Guvakova and Surmacz, 1999; Ridley et al., 2003; Simons and Mlodzik, 2008].

Localized control of actomyosin contractility is essential for directed cell migration. The proper spatial regulation of contraction drives cell migration and determines migration direction [Beningo et al., 2006; Even-Ram et al., 2007; Totsukawa et al., 2004]. Non-muscle myosin II isoforms A and B localize to different cellular regions to regulate traction forces and directionality, respectively, during cell spreading and migration. Myosin activation depends on phosphorylation of myosin light chain (MLC) by Rho kinase (ROCK) and myosin light chain kinase (MLCK) [Ikebe, 2008; Kohama et al., 1996; Ridley et al., 2003; Yoneda et al., 2005]. Cell migration guidance cues coordinate myosin activity by stimulating the RhoA (Rho) GTPase to activate ROCK [Ridley et al., 2003]. Focal adhesion (FA) dynamics are also tightly regulated during directed cell migration [Broussard et al., 2008; Gupton and Waterman-Storer, 2006; Ridley et al., 2003; Totsukawa et al., 2000; Totsukawa et al., 2004]. FAs primarily assemble at the leading edge of the cell and disassemble at the trailing edge of the cell as it moves forward [Broussard et al., 2008]. The proper coordination of adhesion dynamics with actomyosin contractility through spatially-localized regulatory elements is critical to polarized cell migration.

The Abl family kinases, Abl and Arg, regulate actomyosin contractility, adhesion dynamics, and cytoskeletal dynamics [Lapetina et al., 2009; Miller et al., 2004; Peacock et al., 2007; Pendergast, 2002; Zandy et al., 2007]. During integrin-mediated fibroblast adhesion and spreading, Arg localizes to the cellular periphery to promote cellular protrusion, relax actomyosin contractility, and promote FA disassembly [Lapetina et al., 2009; Miller et al., 2004; Peacock et al., 2007]. In response to adhesion, Arg phosphorylates p190RhoGAP (p190) on two tyrosine residues, which promotes binding to p120RasGAP (p120). This activated p120:p190 complex localizes to the cell membrane, where it can inhibit active Rho [Bradley et al., 2006]. Several studies suggest that Abl may also regulate contractility and FA dynamics, possibly by targeting similar substrates as Arg [Antoku et al., 2008; Chen et al., 2009; Lewis and Schwartz, 1998; Salgia et al., 1995; Zandy et al., 2007; Zandy and Pendergast, 2008]. In contrast to Arg, Abl shuttles between the nucleus and cytoplasm [Hantschel et al., 2005; Lewis et al., 1996; Taagepera et al., 1998; Woodring et al., 2003; Yoshida and Miki, 2005]. Their distinct localization suggests that Abl and Arg may exert different spatial control over adhesive and contractile structures.

Here we show that Abl and Arg regulate different zones of contractile and adhesive structures in spreading fibroblasts. *abl*$^{-/-}$ cells exhibit higher FA and stress fiber (SF) staining and lower p120:p190 colocalization in the center of cells relative to wild type (WT) and *arg*$^{-/-}$ cells. In contrast, *arg*$^{-/-}$ cells show higher peripheral FA and SF staining and lower peripheral p120:p190 colocalization relative to WT and *abl*$^{-/-}$ cells. We find that re-expression of Abl-YFP or Arg-YFP in *abl*$^{-/-}$ or *arg*$^{-/-}$ cells, respectively, converts the biased central/peripheral localization patterns into more intermediate, WT-like distributions. The peripheral contractile distribution in *arg*$^{-/-}$ cells leads to significantly stronger collagen gel contractility compared to WT and *abl*$^{-/-}$ cells. Our results indicate that Abl and Arg differentially regulate the spatial distributions of FAs and SFs via the p120:p190-Rho signaling pathway.

Materials and Methods

Constructs

The Arg-YFP expression construct has been previously described [Miller et al., 2004]. The Abl-YFP expression construct was generated using an identical strategy inserting YPF in frame to murine c-Abl type IV via a six amino acid linker.

Cell culture and retroviral infection

The generation of WT and *arg*$^{-/-}$ 3T3 fibroblast lines was described previously [Koleske et al., 1998; Miller et al., 2004]. *abl*$^{-/-}$ 3T3 fibroblasts were generated in a manner similar to the other fibroblasts. Infection of these lines with retroviruses expressing Arg-YFP/Abl-YFP has been described previously [Miller et al., 2004].

Lysate preparation and immunoblot analysis

Lysates were prepared and analyzed by immunoblot as previously described [Bradley et al., 2006; Peacock et al., 2007].

Immunofluorescence microscopy

Cells were plated on glass coverslips coated with 10 μg/ml FN (Sigma-Aldrich) as indicated in the figure legends and blocked with 1% BSA (Gibco/BRL) for the times indicated in the figure legends. Cells were rinsed before fixation with PHEM buffer (60 mM Pipes, 25 mM Hepes, 10 mM EDTA, 2 mM $MgCl_2$, pH 6.9) that was pre-warmed to 37°C. Cells were fixed with 4% PFA (pre-warmed to 37°C) for 20 minutes at room temperature and permeabilized with 0.5% or 1% Triton-X100 for 10 minutes. Cells were stained with antibodies to paxillin (Transduction Labs, cat #610051), phospho-Myosin Light Chain 2 (Ser19) (pMLC) (Cell Signaling, cat #3675/3671), p190-A RhoGAP (C59F7 Rabbit mAb Cell Signaling, cat #2860), p120RasGAP (mAb clone B4F8, Upstate), Alexa 594–labeled or Alexa 488-labeled secondary antibodies (Molecular Probes), followed by Alexa 350-phalloidin (Molecular Probes) to visualize the F-actin cytoskeleton. Cells were imaged on a Zeiss Axioskop microscope equipped with differential interference contrast optics and a Nikon TE2000-S microscope.

Adhesion-dependent RhoA and contractility assays

Adhesion-dependent Rho activity levels were measured as previously described [Bradley et al., 2006] using an enzyme-linked immunosorbent assay (ELISA)-based kit (RhoA G-LISA; Cytoskeleton, Denver, CO). Contractility assays were performed as previously described [Arora and McCulloch, 1994; Peacock et al., 2007].

Quantitation of FAs and SFs

Radial intensity distributions were determined using CellProfiler software [Carpenter et al., 2006; Lamprecht et al., 2007; Vokes and Carpenter, 2008]. Images were taken of cells stained for paxillin, F-actin, p120, p190, or pMLC at 40× magnification. TIFF images were converted to 8-bit grayscale. p120 and p190 were analyzed using the modified NIH ImageJ program created by the McMaster Biophotonics group at McMaster University for colocalization, using the Colocalization highlighter function. Colocalization images were then inverted and used in CellProfiler analysis. CellProfiler analysis involved identifying a nuclear center, outlining the nucleus, and using F-actin brightness/contrast enhanced images to outline the cellular periphery. The radial distribution function was then used to obtain 10 equal bins for the distribution of mean fraction intensity at each bin's distance from the nucleus outwards to the cell periphery. At least 20 cells for each line were analyzed and the means for each bin distance were determined.

Statistical analysis

We used two-factor ANOVA with repeated measures and ANOVA ($\alpha = 0.05$) to compare the multiple groups of data from cells of different genotypes. *post hoc* Student-Newman-Keuls tests were used to determine the statistical significance of the differences between these groups. This test is the most stringent and appropriate to compare two or more unpaired groups.

Results

Abl and Arg localize to different cellular regions in spreading fibroblasts

Previous work has shown that Abl prominently localizes to the nucleus, while Arg localizes to the cell periphery in several different cell types [Koleske et al., 1998; Taagepera et al., 1998; Van Etten et al., 1989; Wang and Kruh, 1996]. Upon retroviral expression of Arg-YFP in *arg*$^{-/-}$ cells (*arg*$^{-/-}$ + Arg-YFP) and Abl-YFP in *abl*$^{-/-}$ cells (*abl*$^{-/-}$ +Abl-YFP), the spatial distribution of Abl-YFP and Arg-YFP reflect these spatial distributions in spreading cells (Fig. 2B and 2C). Abl-YFP localizes to the nucleus, with some residual localization in the cytoplasm (Fig. 2B). In contrast, Arg-YFP localizes solely to the cytoplasm, where it is particularly abundant in a perinuclear region of the cell and at distinct points in the cellular periphery [Miller et al., 2004] (Fig. 2C).

Loss of Abl or Arg function shifts the subcellular distribution of stress fibers and focal adhesions

Our previous work showed that peripheral FAs and SFs are increased in *arg*$^{-/-}$ cells relative to WT cells (Figs. 1A and 1C) [Peacock et al., 2007]. In contrast, *abl*$^{-/-}$ cells contain more and larger FAs and F-actin bundles in the center of the cell than WT or *arg*$^{-/-}$ cells (Figs. 1A-C). We noted that generally the peripheral focal adhesions in *arg*$^{-/-}$ cells are larger, but the peripheral focal adhesions in *abl*$^{-/-}$ cells are smaller and more numerous (Figs. 1A-C). We also found that Abl levels in *arg*$^{-/-}$ cells and Arg levels in *abl*$^{-/-}$ cells are similar to those in control WT cells, indicating that the loss of function of one kinase does not affect levels of the other (Figs. 1D-F). We used CellProfiler image analysis software to quantify the mean intensity for paxillin and F-actin staining at different radial distributions outward from the nucleus toward the cell periphery (Figs. 1G-H) [Carpenter et al., 2006; Lamprecht et al., 2007; Vokes and Carpenter, 2008]. The intensity distributions were broken down into three cell regions: central (comprising the inner 0-40% of the cell's radius from the center of the nucleus out to the cell periphery), medial (comprising the middle 40-80% of the cell's radius from the center of the nucleus out to the cell periphery), and peripheral (comprising the outer 80-100% of the cell's radius from the center of the nucleus out to the cell periphery) (Figs. 1G-H). We utilized these cellular zones, because they corresponded to the general distribution of morphological features within spreading cells. The central (0-40%) region corresponded to the nucleus and peri-nuclear region, the medial (40-80%) region corresponded to the flat, intermediate region in the cell, and the peripheral (80-100%) region corresponded to the more irregular lamellar/lamellipodial region of the cell. Using this analysis, we found that *abl*$^{-/-}$ cells had significantly higher central paxillin staining compared to *arg*$^{-/-}$ cells and significantly higher central F-actin staining compared to WT and *arg*$^{-/-}$ cells (Figs. 1A-C and 1G-H). In contrast, *arg*$^{-/-}$ cells show higher peripheral paxillin and F-actin staining relative to both WT and *abl*$^{-/-}$ cells, while the center of *arg*$^{-/-}$ cells show significantly lower staining intensity for both structures relative to *abl*$^{-/-}$ cells (Figs. 1A-C and 1G-H). WT cells form a ring of FAs and SFs at the border of the medial and peripheral domains, exhibiting significantly higher intensity in this region than either knockout line (Figs. 1A-C and 1G-H).

We next assessed whether retroviral-mediated re-expression of Abl or Arg in *abl*$^{-/-}$ or *arg*$^{-/-}$ cells, respectively, could revert the altered localization of FAs and SFs in these cells (Figs. 2A-C). In each case, we found that Abl-YFP and Arg-YFP were re-expressed at 5-fold over normal WT endogenous levels in *abl*$^{-/-}$ cells (*abl*$^{-/-}$ + Abl-YFP cells) and *arg*$^{-/-}$ cells (*arg*$^{-/-}$ + Arg-YFP cells), respectively (Figs. 2D-F). As hypothesized, *abl*$^{-/-}$ + Abl-YFP cells contained reduced FA and SF intensity in the central/nuclear region and more intensity in the peripheral region compared with *abl*$^{-/-}$ cells (compare Figs. 2B and 2G-H with Figs. 1B and 1G-H). In fact, the FA and SF distribution of these cells exhibited a slightly more peripheral bias than WT + YFP cells, consistent with the modest Abl-YFP overexpression. Similarly, *arg*$^{-/-}$ + Arg-YFP cells contained reduced FA and SF intensity in the peripheral region and more intensity in the internal region compared with *arg*$^{-/-}$ cells (compare Figs. 2C and 2G-H with Figs. 1C and 1G-H). Here, the FA and SF distribution in the *arg*$^{-/-}$ + Arg-YFP cells exhibited a slightly more central bias than in WT +YFP cells, again consistent with the 5-fold Arg-YFP overexpression. Combined with the analysis of the *abl*$^{-/-}$ and *arg*$^{-/-}$ cells reported above, these results suggest that Abl and Arg differentially regulate the spatial distribution of contractile and adhesive structures in spreading fibroblasts, with Abl and Arg attenuating these structures at the cell center and periphery, respectively.

Loss of Abl and Arg coordinately alters spatial localization of p120 and p190 in spreading fibroblasts

The localized assembly of the p120:p190 Rho-inhibitory complex could greatly affect the spatial regulation of both contractility and adhesion. We hypothesized that Abl and Arg may exert their differential effects on FAs and SFs via localization of the p120:p190 complex. In WT cells, p120 and p190 localized to the nuclear region, throughout the cytoplasm, and at the cell periphery, exhibiting a localization pattern intermediate to the two knockout extremes (Figs. 3A-C). We note that p190 is expressed at normal endogenous levels in *arg*$^{-/-}$ and *abl*$^{-/-}$ cells (Figs. 3D-E). We also note that p120 levels in WT and *abl*$^{-/-}$ cells are similar, but that p120 levels are reduced by 20% in *arg*$^{-/-}$ cells (Figs. 3D and 3F). *abl*$^{-/-}$ cells show reduced p120 and p190 staining intensity in regions close to and including the nucleus but increased intensity for both p120 and p190 at the cellular periphery compared to WT and *arg*$^{-/-}$ cells (Figs. 3A-C). In contrast, *arg*$^{-/-}$ cells show almost exclusive nuclear/perinuclear staining for p120 and p190 and very little staining at the cell periphery compared to both WT and *abl*$^{-/-}$ cells (Figs. 3A-C).

Our lab has previously shown that the localization of p190 to the cell periphery requires Arg function [Bradley et al., 2006]. We wanted to determine if p120 localization depended on Abl and/or Arg expression. *abl*$^{-/-}$ + Abl-YFP cells showed a much tighter nuclear/perinuclear distribution of p120 staining compared to the widespread distribution in *abl*$^{-/-}$ cells (compare Fig. S1B with Fig. 3B). *arg*$^{-/-}$ + Arg-YFP cells showed a broader p120 distribution compared to the narrow nuclear p120 distribution of *arg*$^{-/-}$ cells (compare Fig. S1C with Fig. 3C). Quantitative analysis reveals that p120 localization is restored to normal WT distribution in *abl*$^{-/-}$ + Abl-YFP and *arg*$^{-/-}$ + Arg-YFP cells (Fig. S1D). The combined results from Figures 3 and S1 suggest that Abl and Arg regulate spatial localization of both p120 and p190, which are important regulators of Rho signaling pathways.

While the spatial localization of the individual p120 and p190 proteins is important, it is p120:p190 complex formation that is required for Rho inhibition [Bradley et al., 2006]. Therefore, we used NIH ImageJ software to obtain colocalization data for p120 and p190 in the different cell lines (Fig. 3A-C). We again used CellProfiler image analysis software to quantify the mean intensity for p120 and p190 colocalization at different radial distributions outward from the nucleus toward the cell periphery (Fig. 3G). WT cells showed a more

balanced p120:p190 colocalization pattern throughout the cell relative to the two knockout line extremes (Fig. 3G). WT cells had significantly higher p120:p190 colocalization in the central region relative to *abl*$^{-/-}$ cells, but significantly less colocalization in this region compared to *arg*$^{-/-}$ cells (Fig. 3G). At the periphery, WT cells had significantly more colocalization than *arg*$^{-/-}$ cells, but significantly less colocalization than *abl*$^{-/-}$ cells (Fig. 3G). *abl*$^{-/-}$ cells exhibited half the p120:p190 colocalization intensity in the central cellular region and 3.5 times the amount of p120:p190 colocalization at the cell periphery compared with *arg*$^{-/-}$ cells (Fig. 3G). These data suggest a potential role for Abl in promoting p190 and p120 colocalization to a nuclear/perinuclear region, while Arg leads to a broader co-localization pattern within the cytoplasm and at the cell periphery.

We have previously shown that Arg-dependent phosphorylation of p190 promotes its association with p120 and localization to the cell periphery, which is necessary for efficient Rho inhibition. Upon plating on fibronectin, *arg*$^{-/-}$ cells fail to recruit p190 to the periphery and do not engage in proper adhesion-dependent Rho inhibition [Bradley et al., 2006]. In order to determine the role that Abl plays in adhesion-dependent Rho inhibition, we performed similar adhesion assays with *abl*$^{-/-}$ cells. We found that the Rho activity profile of *abl*$^{-/-}$ cells is not significantly different from that of WT cells plated on fibronectin (Fig. 3H). Thus, the redistribution of the p120:p190 complex observed in *abl*$^{-/-}$ cells does not alter total Rho activity levels during initial adhesion and spreading on fibronectin.

Loss of Abl and Arg coordinately alters spatial localization of the contractile apparatus in spreading fibroblasts, leading to differences in cellular contractility

To determine whether the contractile apparatus distribution matches the distributions observed for the F-actin networks, we analyzed the pMLC staining distributions in WT, *abl*$^{-/-}$, and *arg*$^{-/-}$ cells plated on fibronectin (Figs. 4A-D). As hypothesized, the pMLC distribution matches the F-actin distribution for the three cell types. *abl*$^{-/-}$ cells show significant pMLC intensity in the central cellular region relative to *arg*$^{-/-}$ cells, while *arg*$^{-/-}$ cells exhibit lower, central pMLC intensity and higher, peripheral pMLC intensity relative to WT and *abl*$^{-/-}$ cells (Figs. 4A-D). These results suggest that the increased F-actin bundle intensity in the central regions of *abl*$^{-/-}$ cells and peripheral regions of *arg*$^{-/-}$ cells correspond to increased actomyosin contractility in those regions.

We wanted to determine if pMLC localization depended on Abl and/or Arg expression. *abl*$^{-/-}$ + Abl-YFP cells exhibited a much more peripheral distribution of pMLC staining compared to the central distribution in *abl*$^{-/-}$ cells (compare Fig. S2B with Fig. 4B). *arg*$^{-/-}$ + Arg-YFP cells showed a much wider pMLC distribution throughout the cell compared to the peripheral distribution in *arg*$^{-/-}$ cells (compare Fig. S2C with Fig. 4C). Quantitative analysis reveals a close matching of pMLC distributions in *abl*$^{-/-}$ + Abl-YFP and *arg*$^{-/-}$ + Arg-YFP cells relative to pMLC distribution in WT +YFP cells (Fig. S2D). The combined results from Figures 4 and S2 suggest that Abl and Arg regulate spatial localization of pMLC, which consequently regulates cellular contractility.

To test the functional output of the contractile structure distributions that we observed, we utilized collagen gel contraction assays to measure relative contractility among the three different cell lines [Arora and McCulloch, 1994]. We measured the decrease in size of the collagen/fibronectin gels as they were compressed by cell contraction (Fig. 4E). We found that *arg*$^{-/-}$ cells contracted the gels to a greater extent than WT or *abl*$^{-/-}$ cells. These results suggest that the peripheral FA and SF network in *arg*$^{-/-}$ cells is either more primed or more effective at contraction than the analogous networks in WT or *abl*$^{-/-}$ cells.

Discussion

In contrast to the WT cells, both knockouts exhibit significant perturbations of both the adhesion and contractile structures and contractility, which likely impacts their morphology and migration patterns (Figs. 1-4) [Peacock et al., 2007]. We have already observed that the large peripheral SFs of *arg*$^{-/-}$ cells exert increased contractile force on these cells during migration, sliding adhesions along the surface and ripping the cell forward whether adhesions de-adhere or not [Peacock et al., 2007]. Peripheral contractile forces have also been shown to be critical for cell migration [Totsukawa et al., 2004], while internal contractile forces are important for traction force generation and ECM remodeling, but not for cell migration [Amano et al., 2000;Gaggioli et al., 2007;Totsukawa et al., 2004]. Arg counteracts these peripheral structures, cellular contraction, and this rapid migration, which potentially allows for careful, cue-guided cell migration (Fig. 1 and 4) [Peacock et al., 2007]. Here we show that Abl attenuates these same adhesive and contractile structures within the cell interior. The loss of Abl function has a more modest impact on whole-cell contractility than the loss of Arg, although there is a slight increase in cellular contractility relative to WT cells (Fig. 4E). Relaxation of central adhesion and contractility by Abl may promote cell spreading and cell migration. Regulation of these central adhesive and contractile structures may also regulate traction force generation and ECM remodeling.

We show here that the unique localization of Abl to the central, nuclear/perinuclear region and Arg to the cytoplasmic/peripheral region has important, direct consequences on the p120:p190 Rho-inhibitory complex (Figure S3). Abl restricts p120:p190 localization to the nuclear/perinuclear region, while Arg activity leads to a widespread distribution of the complex throughout the cell and at the cell periphery (Figure S3). Localization of the p120:p190 complex to particular regions has important effects on the adhesion and contractile structures in those regions. Abl suppresses internal FAs and SFs in favor of peripheral structures, while Arg helps attenuate these structures at the periphery in favor of a more central distribution. The combined effects of Abl and Arg lead to a tight coordination of p120:p190 complex distribution in WT cells, which controls the spatial localization of FAs and SFs. In migrating cells, careful control of these adhesive and contractile zones is critical for proper migration and directed migration towards cues (Figure S3). Our data suggest that Abl and Arg play important and complementary roles in the spatial regulation of these zones.

Supplementary Material

Refer to Web version on PubMed Central for supplementary material.

Acknowledgments

We thank Xianyun Ye for expert technical assistance, Pam Arora for advice on collagen gel contraction assays, Shannon Gourley and Kevin Collins for helpful discussions, and Michael Koelle for use of his microscope. We thank Chris Mader, Shannon Gourley, and Stacey MacGrath for critical comments on the manuscript. J.G.P. was supported by an NSF Graduate Research Fellowship and an NIH NRSA pre-doctoral award (F31NS062585). This work was supported by NIH grants NS39475 and CA133346 (A.J.K.). A.J.K. is an Established Investigator of the American Heart Association.

References

Amano M, Fukata Y, Kaibuchi K. Regulation and functions of rho-associated kinase. Exp Cell Res. 2000; 261(1):44–51. [PubMed: 11082274]

Antoku S, Saksela K, Rivera GM, Mayer BJ. A crucial role in cell spreading for the interaction of abl PxxP motifs with crk and nck adaptors. J Cell Sci. 2008; 121(Pt 18):3071–82. [PubMed: 18768933]

Arora PD, McCulloch CA. Dependence of collagen remodelling on alpha-smooth muscle actin expression by fibroblasts. J Cell Physiol. 1994; 159(1):161–75. [PubMed: 8138584]

Beningo KA, Hamao K, Dembo M, Wang YL, Hosoya H. Traction forces of fibroblasts are regulated by the rho-dependent kinase but not by the myosin light chain kinase. Arch Biochem Biophys. 2006; 456(2):224–31. [PubMed: 17094935]

Bradley WD, Hernandez SE, Settleman J, Koleske AJ. Integrin signaling through arg activates p190RhoGAP by promoting its binding to p120RasGAP and recruitment to the membrane. Mol Biol Cell. 2006; 17(11):4827–36. [PubMed: 16971514]

Broussard JA, Webb DJ, Kaverina I. Asymmetric focal adhesion disassembly in motile cells. Curr Opin Cell Biol. 2008; 20(1):85–90. [PubMed: 18083360]

Cantley LG. Growth factors and the kidney: Regulation of epithelial cell movement and morphogenesis. Am J Physiol. 1996; 271(6 Pt 2):F1103–13. [PubMed: 8997383]

Carpenter AE, Jones TR, Lamprecht MR, Clarke C, Kang IH, Friman O, Guertin DA, Chang JH, Lindquist RA, Moffat J, et al. CellProfiler: Image analysis software for identifying and quantifying cell phenotypes. Genome Biol. 2006; 7(10):R100. [PubMed: 17076895]

Chen CS. Separate but not equal: Differential mechanical roles for myosin isoforms. Biophys J. 2007; 92(9):2984–5. [PubMed: 17325018]

Chen S, Wang R, Li QF, Tang DD. Abl knockout differentially affects p130 crk-associated substrate, vinculin, and paxillin in blood vessels of mice. Am J Physiol Heart Circ Physiol. 2009

Conti MA, Adelstein RS. Nonmuscle myosin II moves in new directions. J Cell Sci. 2008; 121(Pt 1): 11–8. [PubMed: 18096687]

Elbaum M, Chausovsky A, Levy ET, Shtutman M, Bershadsky AD. Microtubule involvement in regulating cell contractility and adhesion-dependent signalling: A possible mechanism for polarization of cell motility. Biochem Soc Symp. 1999; 65:147–72. [PubMed: 10320938]

Even-Ram S, Doyle AD, Conti MA, Matsumoto K, Adelstein RS, Yamada KM. Myosin IIA regulates cell motility and actomyosin-microtubule crosstalk. Nat Cell Biol. 2007; 9(3):299–309. [PubMed: 17310241]

Friedl P, Gilmour D. Collective cell migration in morphogenesis, regeneration and cancer. Nat Rev Mol Cell Biol. 2009; 10(7):445–57. [PubMed: 19546857]

Friedl P, Brocker EB, Zanker KS. Integrins, cell matrix interactions and cell migration strategies: Fundamental differences in leukocytes and tumor cells. Cell Adhes Commun. 1998; 6(2-3):225–36. [PubMed: 9823473]

Gaggioli C, Hooper S, Hidalgo-Carcedo C, Grosse R, Marshall JF, Harrington K, Sahai E. Fibroblast-led collective invasion of carcinoma cells with differing roles for RhoGTPases in leading and following cells. Nat Cell Biol. 2007; 9(12):1392–400. [PubMed: 18037882]

Gilbert, SF. Developmental biology. 7th. Sunderland, Mass.: Sinauer Associates; 2003. p. 838

Gupton SL, Waterman-Storer CM. Spatiotemporal feedback between actomyosin and focal-adhesion systems optimizes rapid cell migration. Cell. 2006; 125(7):1361–74. [PubMed: 16814721]

Guvakova MA, Surmacz E. The activated insulin-like growth factor I receptor induces depolarization in breast epithelial cells characterized by actin filament disassembly and tyrosine dephosphorylation of FAK, cas, and paxillin. Exp Cell Res. 1999; 251(1):244–55. [PubMed: 10438590]

Hantschel O, Wiesner S, Guttler T, Mackereth CD, Rix LL, Mikes Z, Dehne J, Gorlich D, Sattler M, Superti-Furga G. Structural basis for the cytoskeletal association of bcr-Abl/c-abl. Mol Cell. 2005; 19(4):461–73. [PubMed: 16109371]

Hatten ME. Central nervous system neuronal migration. Annu Rev Neurosci. 1999; 22:511–39. [PubMed: 10202547]

Ikebe M. Regulation of the function of mammalian myosin and its conformational change. Biochem Biophys Res Commun. 2008; 369(1):157–64. [PubMed: 18211803]

Kohama K, Ye LH, Hayakawa K, Okagaki T. Myosin light chain kinase: An actin-binding protein that regulates an ATP-dependent interaction with myosin. Trends Pharmacol Sci. 1996; 17(8):284–7. [PubMed: 8810874]

Koleske AJ, Gifford AM, Scott ML, Nee M, Bronson RT, Miczek KA, Baltimore D. Essential roles for the abl and arg tyrosine kinases in neurulation. Neuron. 1998; 21(6):1259–72. [PubMed: 9883720]

Lamprecht MR, Sabatini DM, Carpenter AE. CellProfiler: Free, versatile software for automated biological image analysis. BioTechniques. 2007; 42(1):71–5. [PubMed: 17269487]

Lapetina S, Mader CC, Machida K, Mayer BJ, Koleske AJ. Arg interacts with cortactin to promote adhesion-dependent cell edge protrusion. J Cell Biol. 2009; 185(3):503–19. [PubMed: 19414610]

Lewis JM, Schwartz MA. Integrins regulate the association and phosphorylation of paxillin by c-abl. J Biol Chem. 1998; 273(23):14225–30. [PubMed: 9603926]

Lewis JM, Baskaran R, Taagepera S, Schwartz MA, Wang JY. Integrin regulation of c-abl tyrosine kinase activity and cytoplasmic-nuclear transport. Proc Natl Acad Sci U S A. 1996; 93(26):15174–9. [PubMed: 8986783]

Miller AL, Wang Y, Mooseker MS, Koleske AJ. The abl-related gene (arg) requires its F-actin-microtubule cross-linking activity to regulate lamellipodial dynamics during fibroblast adhesion. J Cell Biol. 2004; 165(3):407–19. [PubMed: 15138293]

Naumanen P, Lappalainen P, Hotulainen P. Mechanisms of actin stress fibre assembly. J Microsc. 2008; 231(3):446–54. [PubMed: 18755000]

Peacock JG, Miller AL, Bradley WD, Rodriguez OC, Webb DJ, Koleske AJ. The abl-related gene tyrosine kinase acts through p190RhoGAP to inhibit actomyosin contractility and regulate focal adhesion dynamics upon adhesion to fibronectin. Mol Biol Cell. 2007; 18(10):3860–72. [PubMed: 17652459]

Pendergast AM. The abl family kinases: Mechanisms of regulation and signaling. Adv Cancer Res. 2002; 85:51–100. [PubMed: 12374288]

Ridley AJ, Schwartz MA, Burridge K, Firtel RA, Ginsberg MH, Borisy G, Parsons JT, Horwitz AR. Cell migration: Integrating signals from front to back. Science. 2003; 302(5651):1704–9. [PubMed: 14657486]

Russo JM, Florian P, Shen L, Graham WV, Tretiakova MS, Gitter AH, Mrsny RJ, Turner JR. Distinct temporal-spatial roles for rho kinase and myosin light chain kinase in epithelial purse-string wound closure. Gastroenterology. 2005; 128(4):987–1001. [PubMed: 15825080]

Salgia R, Brunkhorst B, Pisick E, Li JL, Lo SH, Chen LB, Griffin JD. Increased tyrosine phosphorylation of focal adhesion proteins in myeloid cell lines expressing p210BCR/ABL. Oncogene. 1995; 11(6):1149–55. [PubMed: 7566975]

Sandquist JC, Swenson KI, Demali KA, Burridge K, Means AR. Rho kinase differentially regulates phosphorylation of nonmuscle myosin II isoforms A and B during cell rounding and migration. J Biol Chem. 2006; 281(47):35873–83. [PubMed: 17020881]

Schmitz AA, Govek EE, Bottner B, Van Aelst L. Rho GTPases: Signaling, migration, and invasion. Exp Cell Res. 2000; 261(1):1–12. [PubMed: 11082269]

Simons M, Mlodzik M. Planar cell polarity signaling: From fly development to human disease. Annu Rev Genet. 2008; 42:517–40. [PubMed: 18710302]

Taagepera S, McDonald D, Loeb JE, Whitaker LL, McElroy AK, Wang JY, Hope TJ. Nuclear-cytoplasmic shuttling of C-ABL tyrosine kinase. Proc Natl Acad Sci U S A. 1998; 95(13):7457–62. [PubMed: 9636171]

Totsukawa G, Yamakita Y, Yamashiro S, Hartshorne DJ, Sasaki Y, Matsumura F. Distinct roles of ROCK (rho-kinase) and MLCK in spatial regulation of MLC phosphorylation for assembly of stress fibers and focal adhesions in 3T3 fibroblasts. J Cell Biol. 2000; 150(4):797–806. [PubMed: 10953004]

Totsukawa G, Wu Y, Sasaki Y, Hartshorne DJ, Yamakita Y, Yamashiro S, Matsumura F. Distinct roles of MLCK and ROCK in the regulation of membrane protrusions and focal adhesion dynamics during cell migration of fibroblasts. J Cell Biol. 2004; 164(3):427–39. [PubMed: 14757754]

Van Etten RA, Jackson P, Baltimore D. The mouse type IV c-abl gene product is a nuclear protein, and activation of transforming ability is associated with cytoplasmic localization. Cell. 1989; 58(4): 669–78. [PubMed: 2670246]

Vicente-Manzanares M, Koach MA, Whitmore L, Lamers ML, Horwitz AF. Segregation and activation of myosin IIB creates a rear in migrating cells. J Cell Biol. 2008; 183(3):543–54. [PubMed: 18955554]

Vicente-Manzanares M, Zareno J, Whitmore L, Choi CK, Horwitz AF. Regulation of protrusion, adhesion dynamics, and polarity by myosins IIA and IIB in migrating cells. J Cell Biol. 2007; 176(5):573–80. [PubMed: 17312025]

Vokes MS, Carpenter AE. Using CellProfiler for automatic identification and measurement of biological objects in images. Curr Protoc Mol Biol. 2008; Chapter 14 Unit 14.17.

Wang B, Kruh GD. Subcellular localization of the arg protein tyrosine kinase. Oncogene. 1996; 13(1): 193–7. [PubMed: 8700546]

Watanabe T, Noritake J, Kaibuchi K. Regulation of microtubules in cell migration. Trends Cell Biol. 2005; 15(2):76–83. [PubMed: 15695094]

Woodring PJ, Hunter T, Wang JY. Regulation of F-actin-dependent processes by the abl family of tyrosine kinases. J Cell Sci. 2003; 116(Pt 13):2613–26. [PubMed: 12775773]

Yang J, Weinberg RA. Epithelial-mesenchymal transition: At the crossroads of development and tumor metastasis. Dev Cell. 2008; 14(6):818–29. [PubMed: 18539112]

Yoneda A, Multhaupt HA, Couchman JR. The rho kinases I and II regulate different aspects of myosin II activity. J Cell Biol. 2005; 170(3):443–53. [PubMed: 16043513]

Yoshida K, Miki Y. Enabling death by the abl tyrosine kinase: Mechanisms for nuclear shuttling of c-abl in response to DNA damage. Cell Cycle. 2005; 4(6):777–9. [PubMed: 15917667]

Zandy NL, Pendergast AM. Abl tyrosine kinases modulate cadherin-dependent adhesion upstream and downstream of rho family GTPases. Cell Cycle. 2008; 7(4):444–8. [PubMed: 18235247]

Zandy NL, Playford M, Pendergast AM. Abl tyrosine kinases regulate cell-cell adhesion through rho GTPases. Proc Natl Acad Sci U S A. 2007; 104(45):17686–91. [PubMed: 17965237]

Abbreviations list

p120	120kD GTPase-activating protein for Ras
p190	190kD GTPase-activating protein for Rho
Abl	Abelson
Arg	Abelson-related gene
Arg-YFP	Arg-yellow fluorescent protein
F-	filamentous
FA	focal adhesion
ArgKI-YFP	kinase-inactive Arg point mutant
MT	microtubule
MLCK	myosin light chain kinase
MLC	regulatory myosin light chain
Rho	RhoA
ROCK	Rho-associated kinase
S.E.	Standard error
SF	stress fiber
pMLC	Ser-19 phosphorylated regulatory myosin light chain
WT	wild type

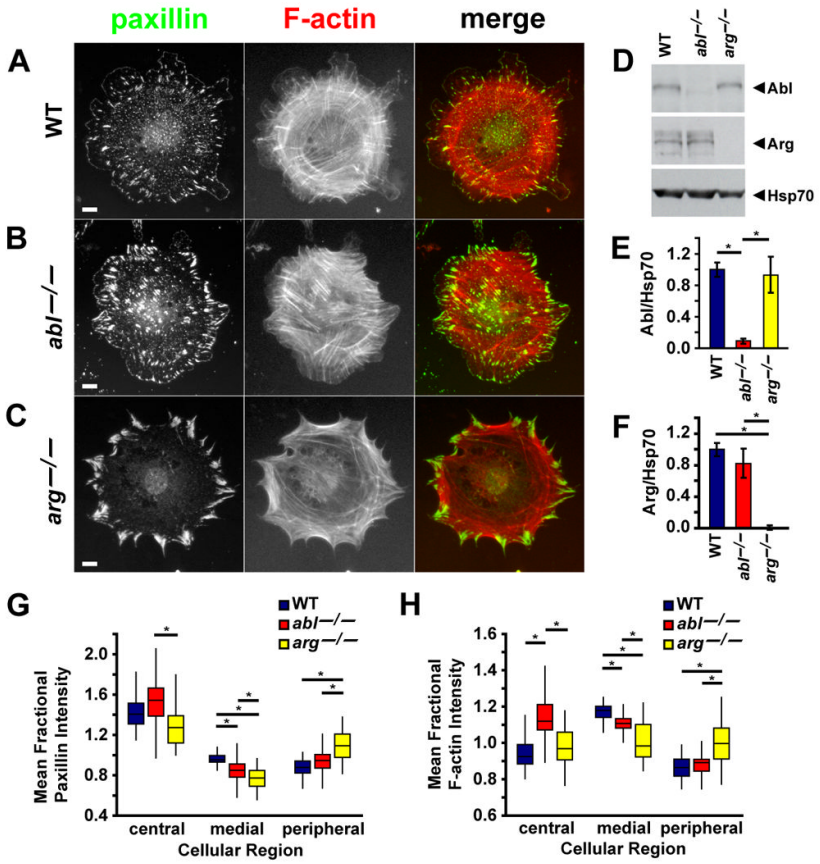

Figure 1. Abl and Arg regulate the localization of focal adhesions and F-actin bundles

(A) WT, (B) *abl*$^{-/-}$, and (C) *arg*$^{-/-}$ fibroblasts were plated on 10 μg/mL FN-coated coverslips, fixed and stained for paxillin and F-actin. Images were obtained with a 40× objective lens. Merged image (merge) shows F-actin (red) and paxillin (green). Bar = 10 μm.

(D-F) Cell lysates (60 μg) of WT, *abl*$^{-/-}$, and *arg*$^{-/-}$ fibroblasts were immunoblotted for Abl, Arg, and Hsp70 (control) (D). Abl levels are similar in WT and *arg*$^{-/-}$ cells, while Arg levels are similar in WT and *abl*$^{-/-}$ cells, n = 4 experiments (E-F).

(G-H) Mean fractional paxillin (G) or F-actin (H) intensity distribution (the fraction of total intensity at a given radial distance) for WT, *abl*$^{-/-}$, and *arg*$^{-/-}$ cells at 0-40% (“central”), 40-80% (“medial”), and 80-100% (“peripheral”) of the radius from the nucleus to the cell periphery. Mean ± S.E. At least 23 cells were analyzed for each genotype and the quantification. Two-factor ANOVA with repeated measures indicated a significant interaction between FA staining distribution and genotype [$F(4,140) = 7.9$, $p < 0.0001$] and between F-actin staining distribution and genotype [$F(4,140) = 16.4$, $p < 0.0001$]. *$p < 0.05$, by post hoc Student-Newman-Keuls.

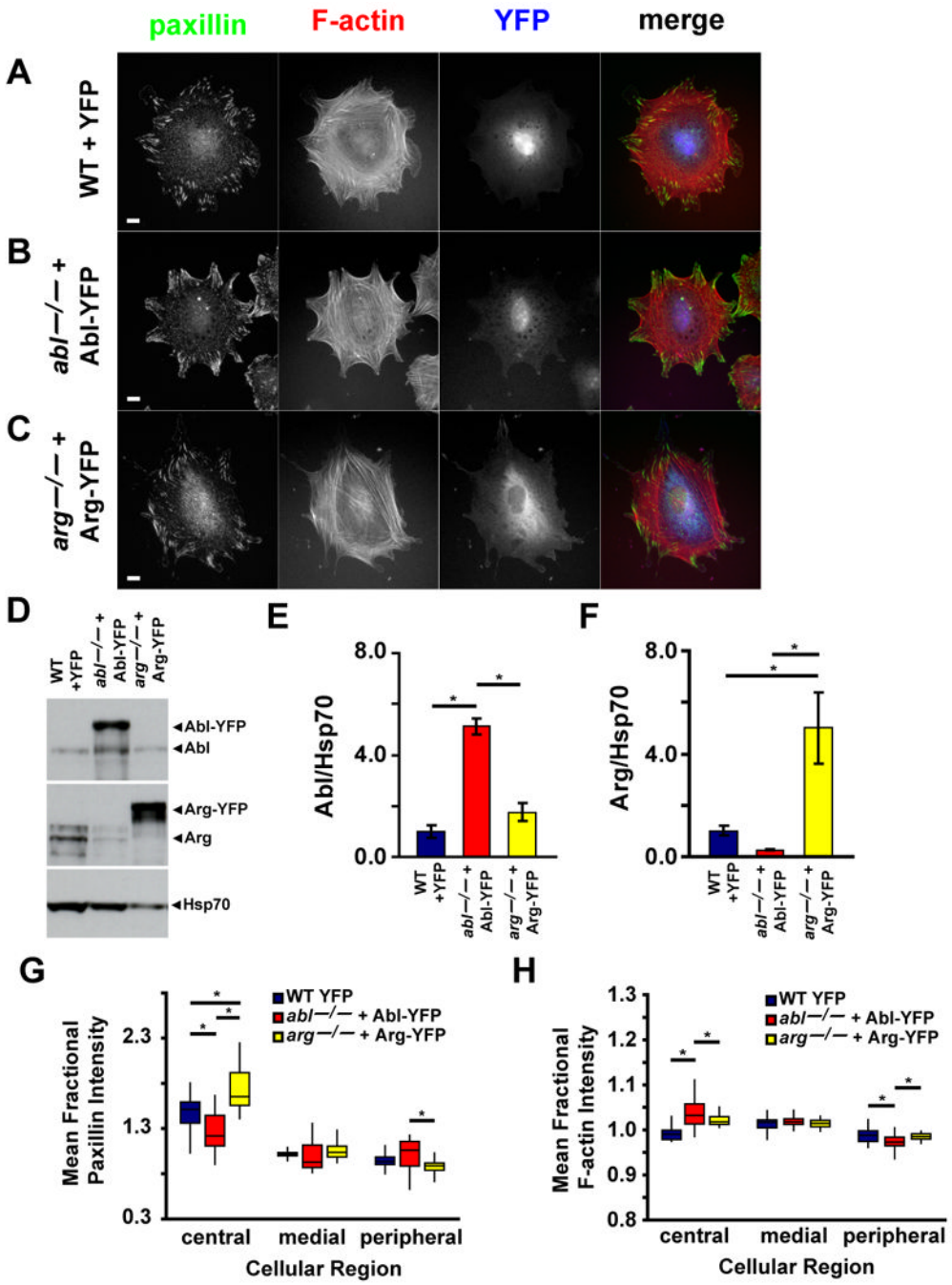

Figure 2. Abl and Arg regulate the spatial localization of focal adhesions and F-actin bundles

(A-C) WT + YFP (A), *abl*$^{-/-}$ + Abl-YFP (B), and *arg*$^{-/-}$ + Arg-YFP (C) fibroblasts were plated on 10 μg/mL FN-coated coverslips for one hour, fixed and stained for paxillin and F-actin. Images were obtained with a 40× objective lens. Merged image (merge) shows paxillin (green), F-actin (red), and YFP (blue). Bar = 10 μm.

(D-F) Cell lysates (60 μg) of WT + YFP, *abl*$^{-/-}$ + Abl-YFP, and *arg*$^{-/-}$ + Arg-YFP fibroblasts were probed for Abl, Arg and Hsp70 (control) (D). Abl-YFP and Arg-YFP levels are 5-fold higher than in WT +YFP cells for both re-expression lines, n = 3 experiments (E-F).

(G-H) Mean fractional paxillin (G) or F-actin (H) intensity distribution (the fraction of total intensity at a given radial distance) for WT + YFP, *abl*$^{-/-}$ + Abl-YFP, and *arg*$^{-/-}$ + Arg-YFP cells at 0-40% (“central”), 40-80% (“medial”), and 80-100% (“peripheral”) of the radius from the nucleus to the cell periphery. Mean ± S.E. At least 21 cells were analyzed for each genotype. Two-factor ANOVA with repeated measures indicated a significant interaction between FA staining distribution and genotype [$F(4,126) = 16.7$, $p < 0.0001$] and between F-actin staining distribution and genotype [$F(4,126) = 7.5$, $p < 0.0001$]. *$p < 0.05$, by post hoc Student-Newman-Keuls.

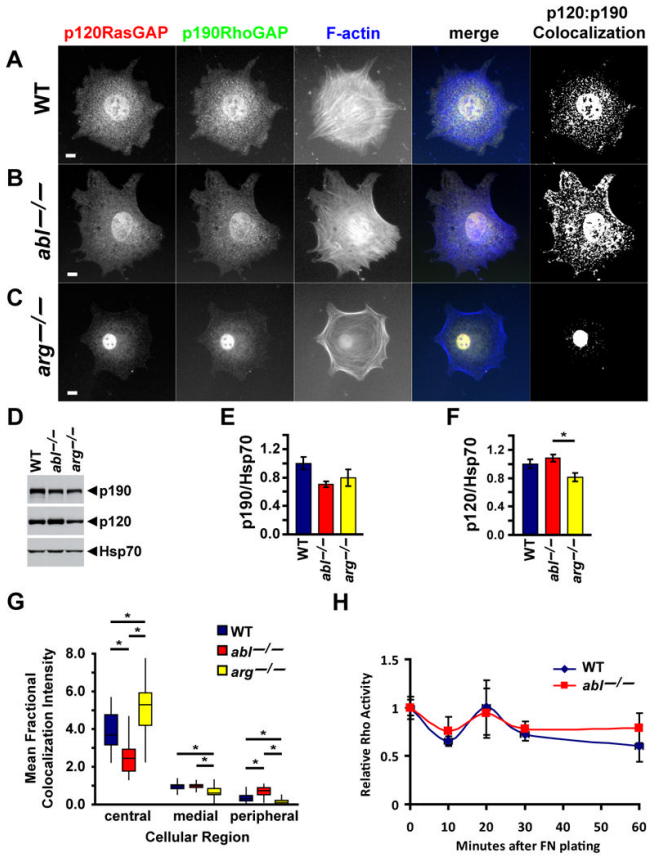

Figure 3. Abl and Arg regulate p120 and p190 colocalization

(A) WT, (B) *abl*$^{-/-}$, and (C) *arg*$^{-/-}$ fibroblasts were plated on 10 μg/mL FN-coated coverslips for one hour, fixed and stained for p120RasGAP, p190RhoGAP, and F-actin. Images were obtained with a 40× objective lens. Merged image (merge) shows p120 (red), p190 (green), and F-actin (blue). NIH ImageJ colocalization image (p120:p190 colocalization) for WT, *abl*$^{-/-}$, and *arg*$^{-/-}$ fibroblasts. Pixels that were above computer-determined threshold values for p120 and p190 are coded white, while other pixels are coded black. Thresholds were set to display the maximal differences in colocalization staining between the cell genotypes. Bar = 10 μm.

(D-F) Cell lysates (30 μg) of WT, *abl*$^{-/-}$, and *arg*$^{-/-}$ fibroblasts were probed for p120, p190, and Hsp70 (control) (D). p190 levels are similar to WT cells for both knockout lines (E). p120 levels are similar for WT and *abl*$^{-/-}$ cells, but p120 levels in *arg*$^{-/-}$ cells are 20% reduced relative to WT and *abl*$^{-/-}$ cells, n = 4 experiments.

(G) Mean fractional colocalization intensity distribution (the fraction of total intensity at a given radial distance) for WT, *abl*$^{-/-}$, and *arg*$^{-/-}$ cells at 0-40% (“central”), 40-80% (“medial”), and 80-100% (“peripheral”) of the radius from the nucleus to the cell periphery. Mean ± S.E. 21 cells were analyzed for each genotype. Two-factor ANOVA with repeated measures indicated a significant interaction between p120:p190 colocalization staining distribution and genotype [$F(4,120) = 23.7$, $p < 0.0001$]. *$p < 0.05$, by post hoc Student-Newman-Keuls.

(H) Rho activity levels were measured in WT and *abl*$^{-/-}$ cells at various times after plating on fibronectin. Points represent mean RhoGTP levels ± S.E., n ≥ 3 for each genotype. Two-factor ANOVA does not show a significant effect of genotype on Rho activity levels [$F(1,29) = 0.3241$, $p = 0.5755$].

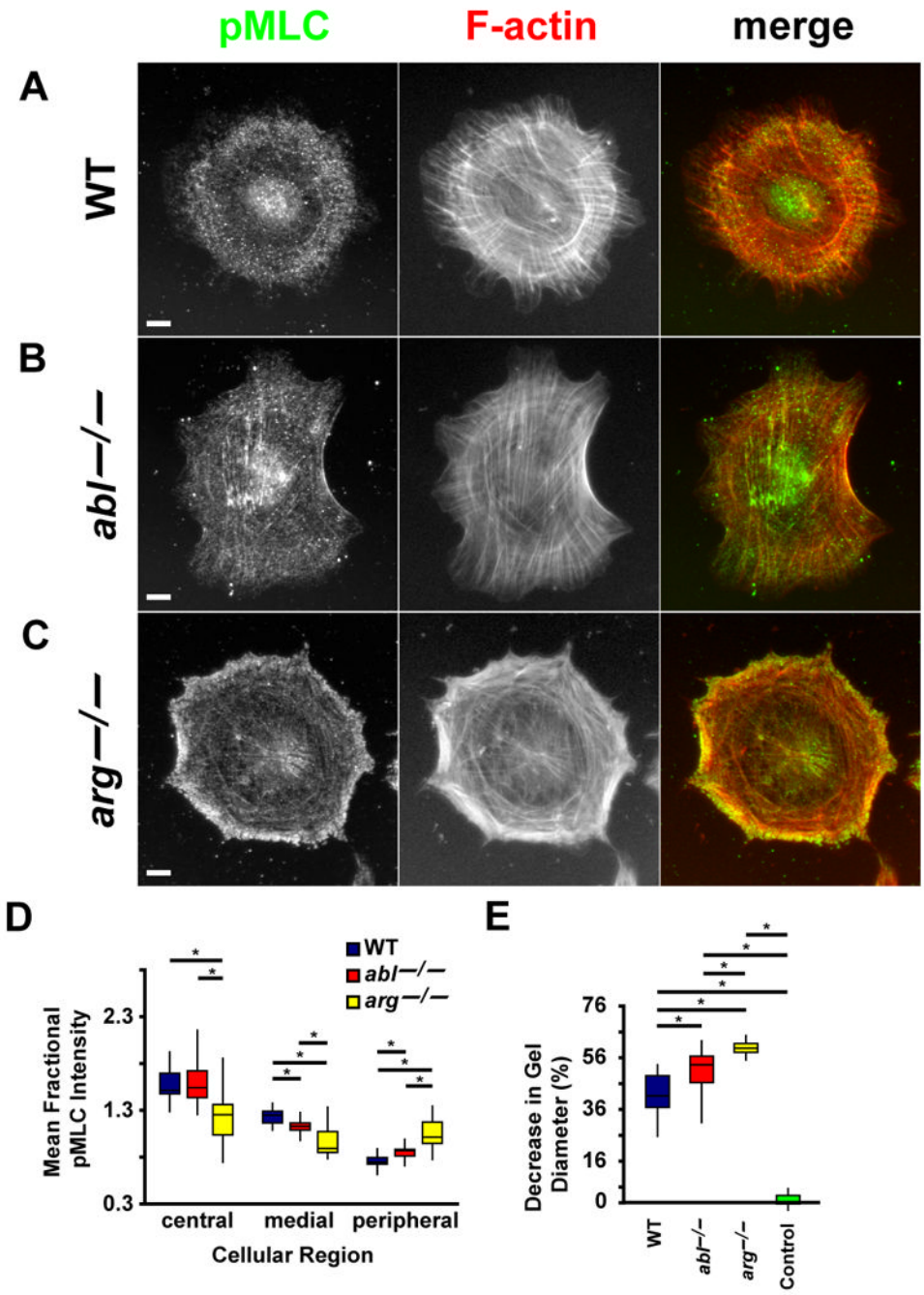

Figure 4. Abl and Arg regulate different zones of the actomyosin contractile apparatus

(A) WT, (B) *abl*$^{-/-}$, and (C) *arg*$^{-/-}$ fibroblasts were plated on 10 μg/mL FN-coated coverslips for one hour, fixed and stained for paxillin and F-actin. Images were obtained with a 40× objective lens. Merged image (merge) shows pMLC (green) and F-actin (red). Bar = 10 μm.

(D) Mean fractional pMLC intensity distribution (the fraction of total intensity at a given radial distance) for WT, *abl*$^{-/-}$, and *arg*$^{-/-}$ cells at 0-40% (“central”), 40-80% (“medial”), and 80-100% (“peripheral”) of the radius from the nucleus to the cell periphery. Mean ± S.E. At least 24 cells were analyzed for each genotype and the quantification. Two-factor ANOVA with repeated measures indicated a significant interaction between pMLC

staining distribution and genotype [$F(4,148) = 22.7$, $p < 0.0001$]. *$p < 0.05$, by post hoc Student-Newman-Keuls.

(E) Contractility of WT, *abl*$^{-/-}$, and *arg*$^{-/-}$ cells collagen/FN gels. The percent decrease in gel diameter is shown for each genotype. The control is a gel with no cells added. Mean ± S.E. 10 experiments for each genotype. ANOVA between data for all genotypes [$F(3,36) = 103.1$, $p < 0.0001$]. *$p < 0.05$, by post hoc Student-Newman-Keuls.